On the biannually repeating slow-slip events at the Ryukyu Trench, southwestern Japan

Kosuke Heki[1] and Takeshi Kataoka[1]

[1] Global positioning system data show that about 20 slow-slip events occurred during 1997–2007 in the southwestern part of the Ryukyu Arc, Japan, where large interplate thrust earthquakes are not known to have occurred in spite of relatively fast plate convergence. They recur fairly regularly on one patch of the subduction fault, which is as deep as 20–40 km and mechanically isolated in an uncoupled subduction zone. They have time constants of a month or so and release seismic moment equivalent of M_w 6.6 on average. This is one of the best recorded sequences of repeating fault slips, with enough events for statistical analyses. They have fairly constant recurrence interval of ∼0.5 year but do not show preferred months of occurrence in a year, suggesting that they are not controlled by seasonal forcing. The correlation between intervals and amounts of fault slip show statistically significant time-predictable recurrences. There is one significant disruption in the rhythm, but the stress perturbations due to nearby earthquakes do not appear to play a significant role. This part of the fault might be an altered asperity that used to rupture fast but now slips only slowly because of the increased ambient temperature.

1. Introduction

[2] Daily measurements of crustal movements by a dense network of global positioning system (GPS) monitoring stations enable us to detect slow movements of faults that do not radiate seismic energy [e.g., *Heki*, 2007]. Plate convergence sometimes takes place as afterslips of large thrust events [e.g., *Heki et al.*, 1997; *Takahashi et al.*, 2004], and such afterslips often show complementary distribution with asperities that ruptured in the main shock [*Yagi et al.*, 2003]. Another kind of slow transient fault motion is slow-slip event (SSE), entirely slow fault rupture that repeats at the plate interface in the transition zone between the smoothly sliding deep zone and the stick-slip shallow zone [e.g., *Hirose et al.*, 1999].

[3] Series of such SSE were found in Shikoku [*Hirose and Obara*, 2005], Southwest Japan, and Tokai [*Ozawa et al.*, 2002] and Boso [*Ozawa et al.*, 2003, 2007; *Sagiya*, 2004] regions, Central Japan. They also occur in the Cascadia subduction zone, western North America [*Dragert et al.*, 2001], in the Guerrero seismic gap, Mexico [*Kostoglodov et al.*, 2003], and possibly in Alaska [*Ohta et al.*, 2007]. Such events are often associated with non-volcanic tremor activities [*Rogers and Dragert*, 2003; *Obara et al.*, 2004], and referred to as episodic tremor and slip (ETS). Now these SSE, together with low-frequency earthquakes [*Ito et al.*, 2006],

are considered to constitute a new category of fault motion governed by its own scaling law [*Ide et al.*, 2007].

[4] It is also known that the recurrences of some of these SSE are fairly regular. For example, events in Cascadia show ∼14 month periodicity [*Miller et al.*, 2002; *Rogers and Dragert*, 2003], and *Shen et al.* [2005] suggested that the periodic stress perturbation by the pole tide may control their recurrences. SSE in Shikoku seems to recur with approximately half year periods [*Hirose and Obara*, 2005]. Mechanisms for these regularities still remain uncertain, due partly to the insufficient number of events for statistical discussions. *Lowry* [2006] suggested that the mechanical weakness of their fault surface makes these SSE susceptible to cyclic external stress perturbations. In fact, tremor activities are found to be highly correlated with semidiurnal and diurnal tides [*Rubinstein et al.*, 2008].

[5] *Yarai et al.* [2004] found repeating SSE in the Ryukyu Arc, southwestern Japan by analyzing the movement of Hateruma, the southernmost island of the arc, from continuous GPS observations. Because one of the fastest convergences in the world occurs there because of the combination of back-arc opening and oceanic plate subduction, SSE with fairly large magnitudes might recur in a relatively short period. Here we study signals of these repeating SSE from the movements at six GPS points on five islands residing on the Southern Ryukyu block during March 1997–December 2007. We investigate these events from various viewpoints, including their time constants, recurrence intervals, consistency between slips and the plate convergence, predictability, triggering by nearby

[1]Department of Natural History Sciences, Hokkaido University, Sapporo, Hokkaido, Japan.
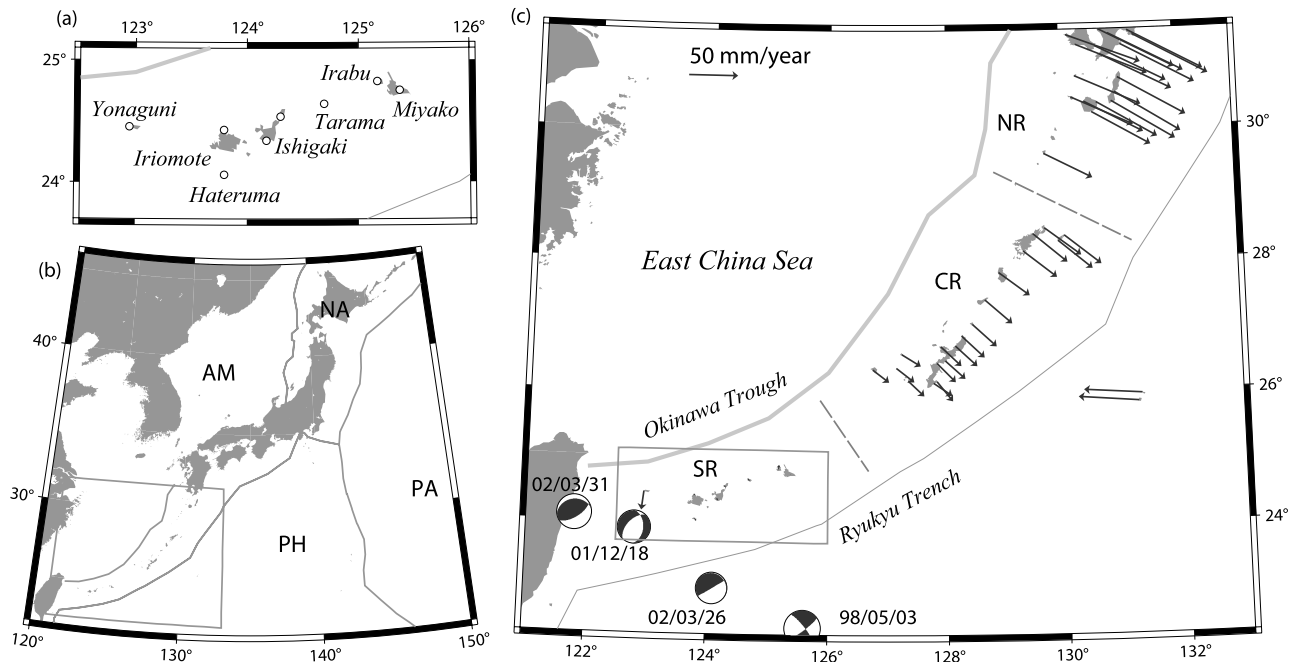
Figure 1. (a) GEONET GPS stations in the South Ryukyu Block of the Ryukyu Arc used in this study (open circles) and the names of the islands. (b) Plate tectonic setting of Japan (NA: the North American Plate, PA: the Pacific Plate, PH: the Philippine Sea Plate, AM: the Amurian Plate). (c) The region between the Ryukyu Arc and the Okinawa Trough moves as three blocks, namely, the Northern Ryukyu (NR), Central Ryukyu (CR), and Southern Ryukyu (SR) Blocks [*Nishimura et al.*, 2004]. GPS velocity vectors are plotted in a frame fixed to SR, and the diminishing size of the arrows in SR shows that little deformation takes place within this block. The squares in Figures 1c and 1b denote the regions shown in Figures 1a and 1c, respectively. Epicenters, focal mechanisms, and dates of four earthquakes that might have influenced deformation transients in SR within the studied time window are shown in Figure 1c.

earthquakes, and so on, in order to shed light on the physics of repeating SSE.

2. Plate Tectonic Setting

[6] At the Ryukyu Trench, SW Japan, the Philippine Sea Plate (PH) subducts toward NW. The overriding Ryukyu Arc shows little interseismic elastic straining, and is composed of three nearly rigid blocks, i.e., North, Central, and South Ryukyu Blocks [*Nishimura et al.*, 2004]. At the Ryukyu Trench south of the South Ryukyu Block (SR) (Figure 1), the plate convergence rate is extremely fast (~12.5 cm/yr) as a consequence of northwestward PH subduction and the southward movement of the arc due to the active back-arc opening at the Okinawa Trough [*Sibuet et al.*, 1998]. Although overall seismic activity is not low, large interplate thrust events are not known at this segment of the plate boundary.

[7] Figure 1c shows the horizontal velocity vectors of GEONET (GPS Earth Observation Network) GPS stations with respect to SR. The velocity vectors, available on line at www.gsi.go.jp/ENGLISH, were obtained by dividing the coordinate differences between the average positions in 1997 and 2007 by ten. Such original velocity fields are aligned to no-net-rotation (nnr)-NUVEL1a [*Argus and Gordon*, 1991] absolute plate motion model, and they were converted into those relative to SR by using a set of Euler vectors obtained by *Nishimura et al.* [2004] using GPS

point velocities. The stations within SR move little with respect to each other, and the lack of interseismic internal deformation is consistent with the absence of large interplate earthquakes at the Ryukyu Trench [*Nishimura et al.*, 2004]. In other words, PH and SR seem to be completely decoupled there.

[8] To the west of this block, in contrast, lies Taiwan where PH collides with the continental lithosphere along the Longitudinal Valley resulting in a large amount of deformation within the island [*Yu et al.*, 1999]. Interplate thrust earthquakes occur at the western extension of the Ryukyu Arc east of Taiwan, and one such event occurred during the study period on 31 March 2002 (M_w = 7.1). The Yonaguni Island, the westernmost island in the study area, is influenced by the interplate coupling there and has a significant velocity relative to SR (Figure 1c). In fact, *Nishimura et al.* [2004] did not use the station on this island to determine the SR Euler vector. The Yonaguni station also moved in association with several large earthquakes in the study period more than other stations, and these movements also contribute to the movement of Yonaguni relative to other stations in SR (Figure 1c).

[9] Figure 2 shows time series of the daily positions of the Hateruma station relative to the Miyako (Gusukube) station (Figure 1a) in the reference frame fixed to SR. There are a few jumps in the time series corresponding to nearby earthquakes (Figure 1c). Apart from them, the secular trend in the time series is small reflecting little internal deforma-
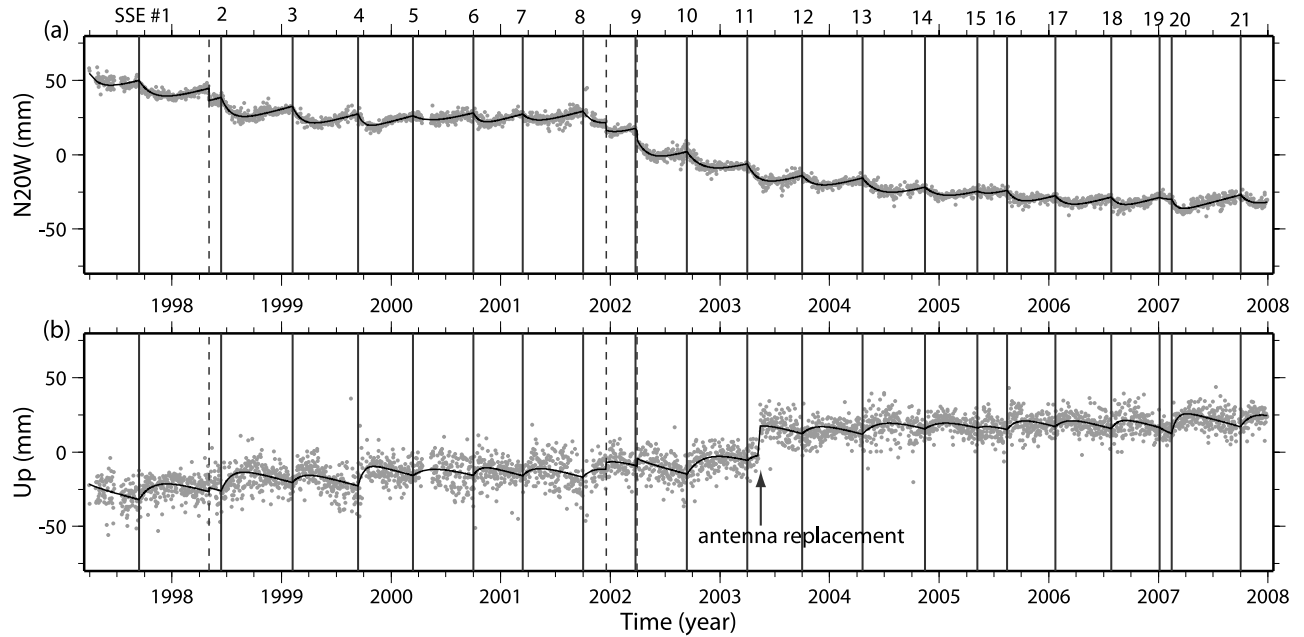
Figure 2. The daily displacements (gray circles) of the GPS station on Hateruma Island (Figure 1a) relative to the station on Miyako Island (Gusukube) in the (a) N20W and (b) up directions. Solid vertical lines show the onset times of the 21 slow-slip events (SSE), and the broken lines indicate earthquakes shown in Figure 1c (the two earthquakes on 26 and 31 March 2002, overlap with the 9th SSE). Solid curves indicate the models based on equation (1). A step in 2003 seen in the vertical component is due to the antenna replacements. SSE numbers are given at the top.

tion of the block. As reported by *Yarai et al.* [2004], the time series includes signatures of SSE characterized by relatively sharp drops followed by slow recovery in the N20W component (Figure 2a). Synchronous sharp uplift and slow subsidence are seen in the up component as well (Figure 2b). Unfortunately, the Japanese high-sensitivity seismometer network has not been extended to these islands yet, and it is unknown if non-volcanic deep tremor activities accompany these event.

3. Observed Slow-Slip Events

3.1. Model for the Coordinate Time Series

[10] Twenty-one SSE were found by close visual inspection. In Figure 3 we replot the time series in Figure 2a but separate the SSE and line up their onset times. The movements in individual SSE are fairly similar. They all feature rather rapid initial negative changes (i.e., movements toward N70E) of 10–15 mm followed by slow reverse motion until the next event. We modeled the coordinate x in an arbitrary component at time t as,

$$x = at + b + \sum_{i=1}^{n} X_i \left[1 - \exp \frac{-(t - T_i)}{\tau_i} \right] \quad (T_1 < T_2 < \cdots < T_n < t),$$

(1)

where b is the simple offset, and the long-term trend a is the background velocity that brings the coordinate back to the pre-event position. This long-term velocity corresponds to the interseismic crustal movements and was assumed constant throughout the studied period. Time constants for

the i'th SSE, denoted as τ_i in (1), ranged from 0.10 to 0.15 years. The SSE start at $(T_1, T_2, T_3, \ldots, T_n)$, and X_i is the displacement of the i'th SSE achieved after a very long time. Actually, between-event intervals are much longer than the time constants, and this "final" displacement is almost achieved, i.e., the value in the parenthesis in (1) becomes almost unity (>0.99 in most cases) before the next event starts. The number of SSE before the time t is given as n, and this increases with time. The time constants τ_i were determined by grid search for individual events using the N20W movement of the Hateruma station, the component with the best signal-to-noise ratio.

[11] The start and decay of each slip in these events seem to be simultaneous at all stations and for all components. In Figure 3b we compare the time series before and after the 2nd SSE at five GPS stations whose locations span ~100 km along the arc. If the rupture propagated as slowly as 13 km/day in Shikoku [*Obara*, 2002], 6 km/day in Cascadia [*Dragert et al.*, 2001], or 0.6 km/day in Guerrero, Mexico [*Lowry et al.*, 2001], there would be a difference of at least a week in the onset times at these points. This is not the case, i.e., a large portion of the fault seems to move coherently in every event. In this study, the same onset times and time constants were used to estimate X_i for individual components and stations using the least-squares method. Among the twenty-one events, the 19th SSE seems peculiar in that the next (20th) event occurred only ~0.1 year later. The 15th event has a clear decaying signature, but its short duration did not allow its time constant to be constrained. For these two events, the time constants (τ_{15} and τ_{19}) are both assumed to be 0.1 year.
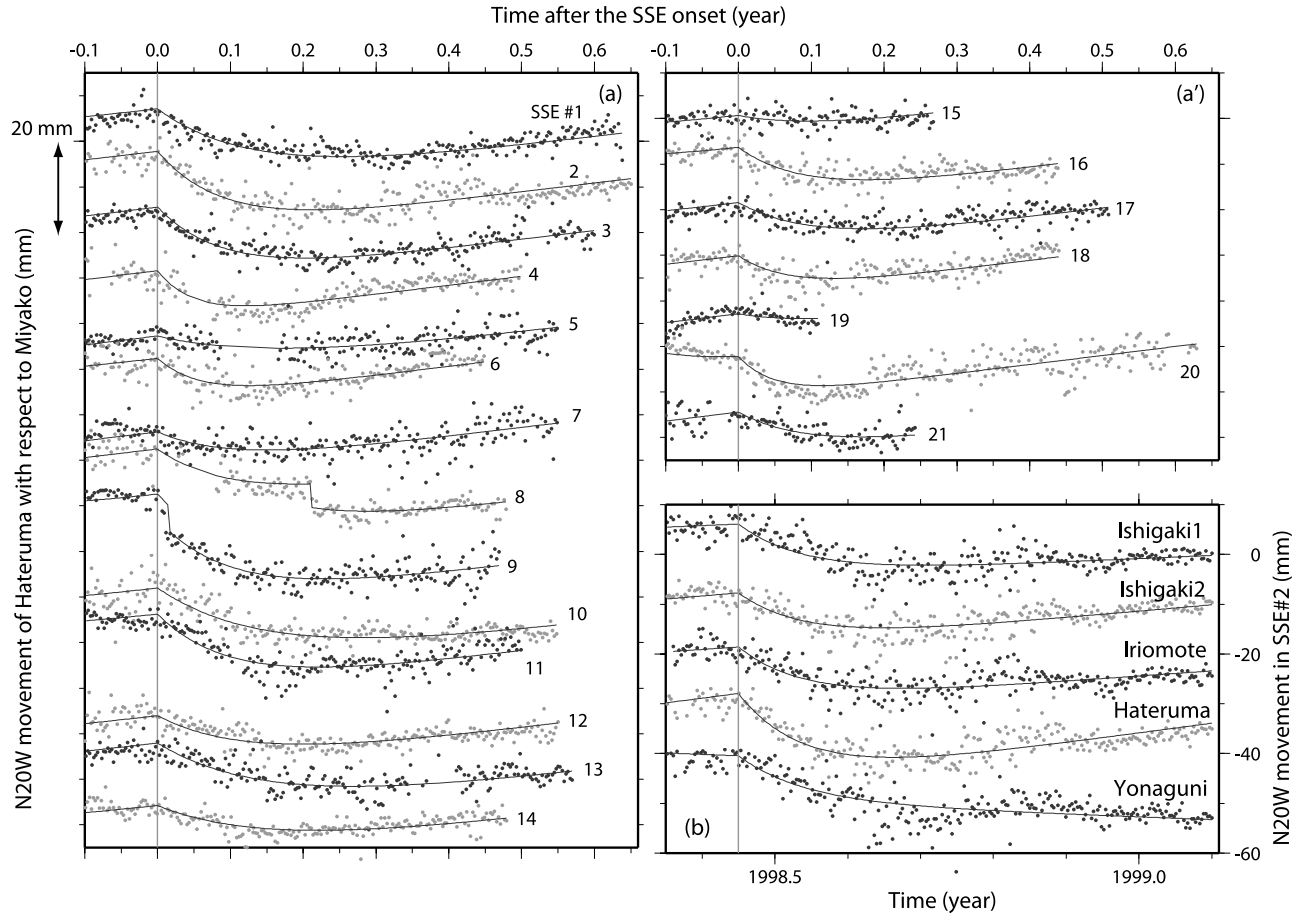
Figure 3. (a) The same time series as in Figure 2a (daily N20W displacements of Hateruma) are shown by plotting individual SSE numbers separately with the origin at their onset times. Difference in the darkness of the gray symbols is for visual clarity. Gray curves are model curves based on equation (1). SSE numbers (Figure 2) are labeled on each event. (b) Daily N20W coordinates of five different GPS sites for the same SSE (2nd) are compared to show the coherence of movements at these sites. If the rupture propagated at a rate 6 km/day as in Cascadia [*Dragert et al.*, 2001], it would take ~2 weeks for the rupture to propagate between Ishigaki and Yonaguni (separated by ~100 km).

[12] In the vertical time series, a jump was caused by the antenna replacement in May 2003. Antennas in these island stations were replaced one after another over a week, i.e., 7–13 May 2003. We exclude the data in this period from later discussions, and we estimated and corrected jumps in coordinates to accommodate these discontinuities. Coseismic jumps were estimated for the three earthquakes that occurred during the studied time interval (3 May 1998, 18 December 2001, and 31 March 2002, see Figure 1c for locations and mechanisms, and Figure 2 for times). For the Mar. 26 2002 earthquake, no significant coseismic steps were observed at any points.

3.2. Estimation of the Fault Parameters

[13] Next we estimate parameters of the fault patch that moved in individual SSE. Instead of the theoretical final displacement X_i, we use the actual final displacement X_i'

$$X_i' = X_i\left[1 - \exp\frac{-(T_{i+1} - T_i)}{\tau_i}\right], \tag{2}$$

which is the maximum displacement in the i'th event achieved until the $(i + 1)$'th event starts. In most cases, X_i' is almost identical to X_i, with the difference less than one percent. However, when the interval after an event is relatively short, X_i' becomes smaller than X_i. This shortage is ~7 percent for the 15th event, but reaches ~33 percent for the 19th event.

[14] Figure 4 shows the 17th SSE that occurred in early 2006 as a typical example. The horizontal (Figure 4a) and vertical (Figure 4b) displacements at six GPS stations (obtained as X_i' in equation (2)) were well explained by a uniform slip of ~6 cm of a rectangular fault plane as large as ~70 km × ~90 km, striking N70E and dipping 15 degrees toward NNW. Its upper and lower edges were estimated as 20 and 40 km, respectively. We calculated the surface displacements due to fault dislocations assuming an elastic half space according to *Okada* [1992].

[15] The two components of the fault dislocation vector were estimated using the least-squares method from the three-dimensional displacements at the six GPS stations.
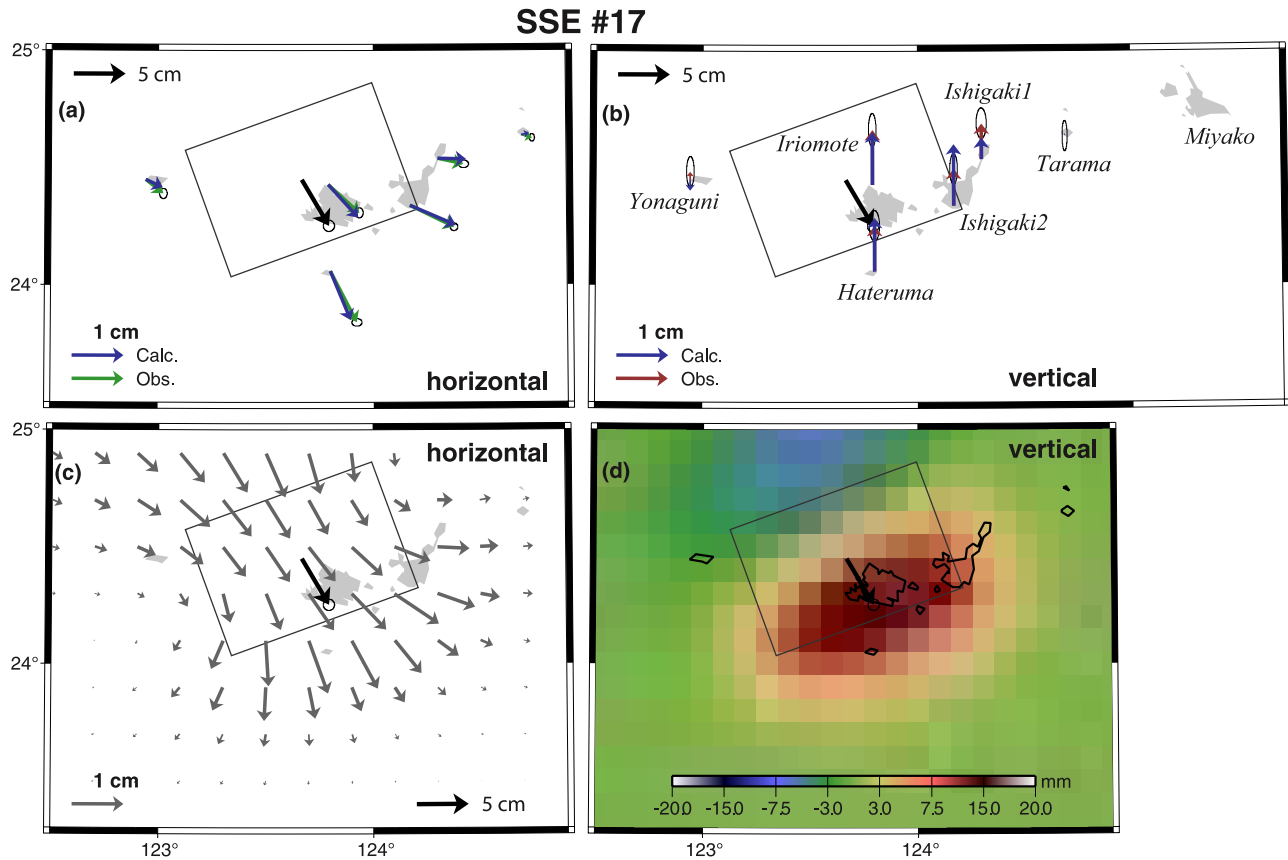
Figure 4. The estimation of the fault patch that moved in the 17th SSE using the observed horizontal (green arrow in Figure 4a) and vertical (red arrows in Figure 4b) displacements. The fault patch is centered at 24°27′N 123°47′E and at depth of 32 km, and its dimension is 94 km in length and 66 km in width. It dips 15° toward NNE with strike 250°. Blue arrows in Figures 4a and 4b are the displacement vectors calculated using the fault slips shown by the black arrow. We used the model by *Okada* [1992]. Calculated horizontal and vertical displacements at grid points are given in Figures 4c and 4d, respectively.

Geometric parameters such as center coordinates of fault patch, fault width/length, dip, strike, and depth were optimized by grid search to realize the smallest post-fit residuals. Among these parameters, horizontal positions are relatively well constrained with the given GPS site distribution. The data were, however, less sensitive to the size (width and length), dip angle, and vertical position of the patch. Nevertheless, we could constrain them without major problems for the 17th SSE (Figure 4), and we used the same fault plane for all the SSE just allowing the difference in the sizes of the patch that slipped.

[16] Figures 4c and 4d suggest that Miyako (see Figure 4b for location) does not move because of this fault movement, which justifies our approach to fix it as the reference. The fault model well explains the diverging horizontal movement of the Iriomote, Ishigaki, and Hateruma Islands toward SSE and their uplift. Tarama and Yonaguni stations move little, which is also consistent with the model. Because the GPS site distribution is limited, non-uniform slip distribution cannot be resolved. Here we assume a uniform slip over the slipped patch. The depth of the fault patch (∼30 km at the center) suggests that the actual plate

boundary may be somewhat shallower than the isobaths of the Wadati-Benioff zone there determined using horizontal locations and depths of earthquakes [*Sibuet et al.*, 1998].

[17] Figure 5a shows horizontal displacements and estimated fault slips for all the 21 events. Similar GPS site and fault displacement vectors to the 17th SSE signals (Figure 4a) are seen for them although the scale varies slightly from event to event. Such similarity suggests that slow ruptures occur at the same part of the PH-South Ryukyu boundary repeatedly. Although we assumed the same fault patch size as the 17th SSE for the majority of the events, we slightly modified the along-arc ends of the fault for some of the events. For example, four SSE (1st, 2nd, 9th, and 10th) showed somewhat different displacement patterns; Ishigaki12 and Yonaguni showed longer displacement vectors than others. A revised fault geometry with extension by 20 km in both directions resulted in better fit to the observed displacements. For the 3rd and 14th events, we extended the fault by 20 km only for the WSW side to explain larger movements at Yonaguni.

[18] At the end of Figure 5a, we show the background velocity (*a* in equation (1)) vectors. They trend almost
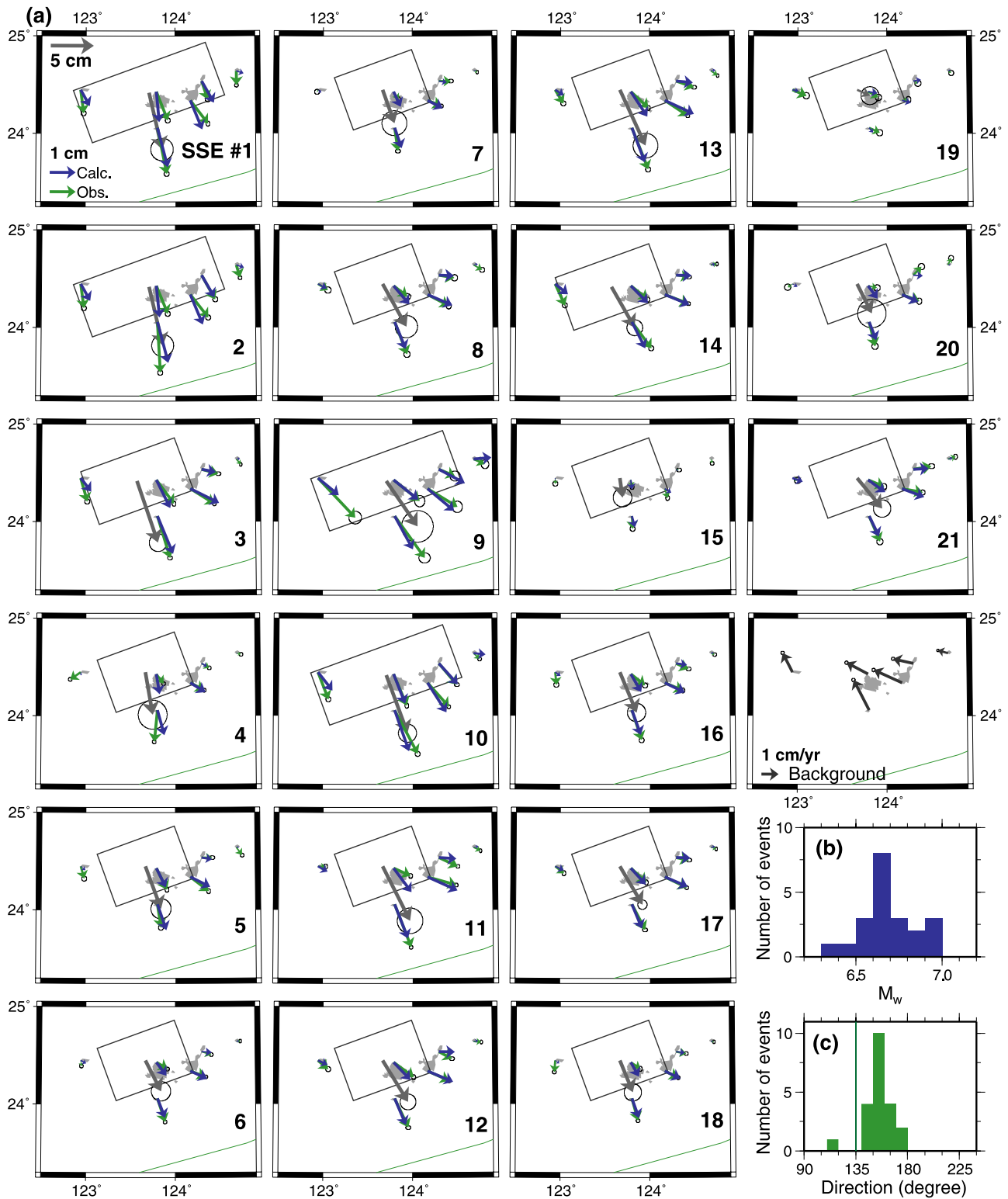
Figure 5. (a) Horizontal displacement vectors (blue/green arrows) and estimated fault slips (gray arrows) for the 21 SSE studied here. Error ellipses indicate 2σ. For SSE 1, 2, 9, and 10, we extended the fault length by 20 km in both directions. For SSE 3 and 14, the extension was done only toward WSW. For the other events, the same fault as in Figure 4 is assumed. Below the panel for the 21st SSE, we show the background velocity vectors (black arrows) estimated as a in equation (1) (for the Yonaguni station, its time-averaged velocity shown in Figure 1c is subtracted to isolate interseismic velocity). (b) Histogram showing the distribution of moment magnitudes. (c) Histogram of slip azimuths showing a systematic clockwise deviation by $\sim 20°$ from the predicted plate convergence direction (134°) (the green line).
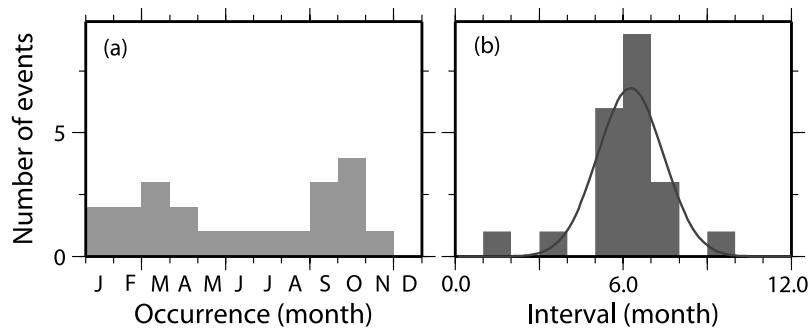
Figure 6. (a) Histograms showing the distribution of the occurrence months of SSE, where two vague peaks are seen in March and October. (b) Histogram of recurrence intervals showing a strong peak at half year. The average interval is 6.3 months, with the standard deviation ∼1.2 months (∼0.10 yr) if the data are fitted with a Gaussian distribution, as shown by the gray curve (an exceptionally short time interval after 19th SSE, ∼2 months, is excluded from the calculation of the mean and standard deviation).

opposite to the displacements by SSE, and demonstrate the existence of interseismic elastic straining by the coupling at depth which was invisible in long-term average velocity fields (Figure 1c). The original concept of little deformation within SR [*Nishimura et al.*, 2004] is correct for the timescale of years or longer, but is not true for velocity fields with time resolution better than a half year. For the 9th SSE, there is an excess southeastward movement of Yonaguni, and this is due to the afterslip of the 26 March 2002 earthquake near Taiwan. We will discuss this point later.

3.3. SSE and Plate Convergence

[19] The average slip in each SSE is 5−6 cm (Figure 5). If we multiply this with the average recurrence interval of half a year, we obtain a value similar to the model plate convergence rate of ∼12.5 cm/year. Their slip directions, however, deviate by ∼30 degrees clockwise from the model direction of 134° (Figure 5c). This might reflect the error in SR Euler vector estimated by *Nishimura et al.* [2004]. Interplate earthquakes provide directional information on relative plate motion at boundaries. However, large earthquakes do not occur there, and they had to rely on GPS point velocities occupying only a portion of the block to estimate the Euler pole. This is reflected in the NW−SE elongation of the error ellipse of the SR Euler pole, located east of the block, i.e., the slip direction is not as well constrained as the convergence rate [Figure 9 of *Nishimura et al.*, 2004].

[20] The seismic moment of these SSE, obtained using the slip areas and values (we assumed rigidity of 40 GPa), had an average value equivalent to M_w ∼6.6 (Figure 5c). This magnitude and their time constants of 0.10−0.15 years are consistent with the general scaling law for slow earthquakes proposed by *Ide et al.* [2007]. The average magnitude and time constants are similar to those of ETS in Cascadia (typical M_w is 6.7, with time constants 2−4 weeks [*Miller et al.*, 2002; *Dragert et al.*, 2004]), but the average recurrence interval (∼6 month) is much shorter than in Cascadia (∼14 month) perhaps reflecting the faster plate convergence than in Cascadia (∼3.7 cm/yr). One large difference is that the rupturing area migrates over three

weeks with the speed ∼6 km/day in Cascadia [*Dragert et al.*, 2001], but the whole fault patch moves coherently in Ryukyu.

4. Recurrence of Slow-Slip Events

4.1. Recurrence Interval and Apparent Seasonality

[21] Many SSE are known to repeat fairly regularly. For example, ETS in Cascadia occur quasi-periodically every ∼14 months [*Miller et al.*, 2002; *Rogers and Dragert*, 2003]. Those in Shikoku seem to occur every half year [*Hirose and Obara*, 2005], and slow events in Guerrero, Mexico, occur mainly in the winter [*Lowry*, 2006]. The occurrence times of the SSE in South Ryukyu seem to have a weak peak in spring and autumn (Figure 6a), i.e., twelve events occur in four months, March, April, September, and October. This may reflect the existence of certain external cyclic forces, such as the pole tide proposed for Cascadia [*Shen et al.*, 2005], and hydrological load proposed for Mexico [*Lowry*, 2006]. On the other hand, the half-year average recurrence may simply be a coincidence and have nothing to do with seasonality. In South Ryukyu we have records of 21 SSE occurrences, which offers a chance to distinguish between two possibilities, (1) they just repeat with an internal rhythm with ∼1/2 year recurrence, or (2) they are controlled by an external seasonal forcing.

[22] An important feature of the Ryukyu SSE is that they have a strong peak in the recurrence interval at ∼1/2 year (6.3 months on average with standard deviation 1.2 months) (Figure 6b). If possibility A is correct, there would be no external force to bring the occurrence time to "right" season once the regularity breaks down e.g., by an event after an exceptionally short recurrence period. In fact, the events occur in spring and autumn in 2000, but they occur in winter and summer in 2006. Such a lack in consistency favors A.

[23] In the case B, occurrence times of the events were assumed to have a Gaussian distribution around the two epochs in a year, middle March and middle September. In this case, peaks should be clear in both of the histograms with the peak of the recurrence interval being $\sqrt{2}$ times as broad as that of the occurrence time. This is clearly not the
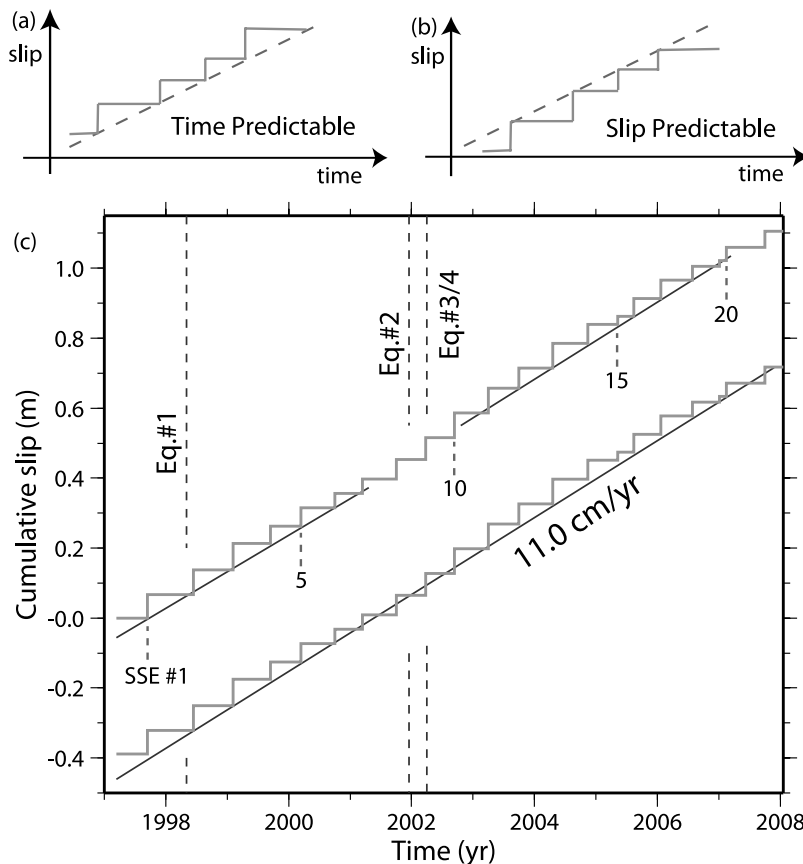
Figure 7. If recurrences are (a) time or (b) slip predictable, the lower right or upper left corners, respectively, of cumulative slip diagrams are expected to align. (c) Cumulative slip by the SSE 1997–2007 in the Ryukyu Arc. The vertical positioning of the lines is arbitrary. Their lower edges align, suggesting time-predictable recurrence of the SSE. Here two cases are shown, i.e., (upper) two straight lines were fitted to the earlier and later halves of the data excluding the period covering 8th to 10th SSE, and (lower) one line is fitted to all the data. The fit becomes poor in the middle of the time span, whose causal relationship with nearby earthquakes (Figure 1c) is discussed in the text. The gradient of the fitted lines is identically 11.0 cm/yr, which is close to the plate convergence rate there.

case, i.e., the observed weak seasonality in the occurrence time would be due simply to nearly biannual occurrence of the events. SSE with various recurrence intervals have been found, e.g., those in Boso, Kanto District, Japan, occurred in 1996, 2002, and 2007 [*Ozawa et al.*, 2003, 2007] with a 5–6 years periodicity. SSE in Tokai, Central Japan [*Ozawa et al.*, 2002], are suggested to occur with recurrence intervals longer than a decade [*Yamamoto et al.*, 2003]. Such diversity suggests that the six months interval studied here does not have a special geophysical meaning.

4.2. Correlation Between Recurrence Intervals and Fault Slips

[24] The recurrence intervals have a standard deviation of 1.2 months around its mean (Figure 6b). The amounts of slip also have certain scatter (Figure 5b). Here we evaluate the correlation between the two quantities. *Shimazaki and Nakata* [1980] suggested two end-member types of correlation, referred to as the time- and the slip-predictable models (Figures 7a and 7b). In the former, recurrence time is proportional to the magnitude of the previous event. The explanation is that the maximum stress is constant while the stress drops vary from event to event. In the latter, the magnitude is proportional to the time elapsed since the last event. The explanation is that events let the stress drop to a constant value while the rupture may occur at any stress level.

[25] Here we consider correlation between slips and the recurrence intervals following and preceding slips. Significant correlation would imply the time- or slip-predictability, respectively. The correlation coefficients (0.83 and 0.40, respectively) suggest that the slips correlate more with the interval after the events than those before the events, suggesting that the recurrences are more time-predictable. The relatively small span of the recurrence interval distribution makes it rather difficult to draw a definitive conclusion on this matter. For example, 19th SSE is peculiar in several points and the correlation decreases from 0.83 to 0.64 by excluding this event. This value, however, still indicates a significant positive correlation between the two quantities. On the other hand, the correlation coefficient 0.40 for the slip-predictable case is not significant at the 95 percent confidence level. After all, these SSE seem to recur in a time-predictable manner
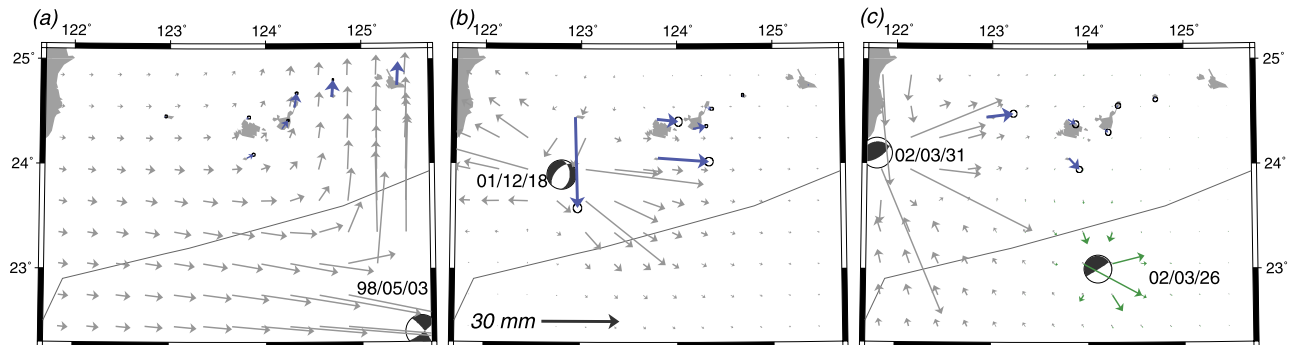
Figure 8. Coseismic movements of GPS stations associated with the four relatively large earthquakes are drawn by blue arrows for events in (a) 1998 May 3, (b) 18 December 2001, and (c) 26 March 2002. The movements of Miyako, used as the fixed reference in obtaining displacements in SSE, were fixed to the calculated vectors (significantly different from zero in the 1998 earthquake). In Figure 8a, observed displacements are consistent with the predicted vectors (light gray). On the other hand, those in Figures 8b and 8c are smaller than predicted (directions are consistent with predictions), suggesting the existence of significant afterslips. In Figure 8c, predicted vectors by another earthquake in 26 March 2002, are shown with green arrows.

usually, and departure from the model occurs sometimes as discussed in the next section.

5. Discussions

5.1. Stress Disturbances by Regular Earthquakes and Recurrence Rhythms

[26] If the recurrence is time-predictable, the lower-right corners of cumulative slip diagram should align (Figure 7a). This is almost the case, i.e., they align in the two time windows 1997–2001 and 2002–2007, but the linearity breaks down in the middle of the time series around 2001–2002 (around 8th and 9th SSE) (Figure 7c). The slope of the best-fit line of these corners is ~11.0 cm/yr, which is close to the plate convergence rate ~12.5 cm/yr at this boundary. Then the interseismic (inter-slip, actually) plate coupling is nearly full at this segment.

[27] Here we discuss if the breakdown has anything to do with four nearby earthquakes that occurred during the study period (Figure 1c). Four large earthquakes occurred during this period, (1) 3 May 1998 23:30UT, $M_w = 7.5$, (2) 18 December 2001 04:03UT, $M_w = 6.7$, (3) 26 March 2002 03:46UT, $M_w = 6.4$, and (4) 31 March 2002 06:53UT, $M_w = 7.1$. In Figure 8 we compare observed coseismic movements in these earthquakes together with those predicted by the fault parameters from seismological studies [Y. Yamanaka, Nagoya University, http://www.eri.u-tokyo. jp/sanchu/Seismo_Note]. There we assumed an elastic half space [Okada, 1992].

[28] Among them, only the earthquake (4) in Taiwan is an interplate thrust earthquake while others are intraplate events with various mechanisms. Earthquake (1) is a relatively large strike-slip event within the subducting oceanic plate, and the observed coseismic jumps are consistent with those calculated (Figure 8a). Earthquake (2) is a shallow normal fault event possibly related to the backarc opening at the Okinawa Trough. For this event, the directions of the observed movements agree more or less with the predictions, but the observed vectors are too large (Figure 8b). This might be due to afterslip that followed the fast rupture.

[29] The earthquake (4) is an interplate thrust event at a western extension of the Ryukyu Trench near Taiwan, and a clear coseismic step is seen in Yonaguni (Figure 8c). Again, the observed coseismic movement is a few times as large as the prediction, suggesting the possible existence of significant afterslip (time series of Yonaguni in Figure 9 show afterslip signatures). Although Figure 8c shows that there are coseismic displacements at Hateruma and Iriomote, the time series in Figure 9 do not show clear coseismic steps associated with this earthquake. Because the earthquake (4) and the 9th SSE are separated in time by less than a week, it is difficult to separate their GPS signals. Hence a part of the Yonaguni displacement in the 9th SSE (Figure 5a) would be actually from the earthquake (4), and a part of the Hateruma/Yonaguni coseismic displacement in the earthquake (4) (Figure 8c) would be the leakage from the 9th SSE.

[30] Although no stations showed coseismic jumps for the earthquake (3), the 9th SSE started simultaneously with this earthquake suggesting possible causal relationship between them. We calculated the increase of Coulomb Failure Stress (ΔCFS) for a thrust faulting of the fault patch shown in Figure 4. We first calculated the strain tensor at the fault center following Okada [1992], and converted the coordinate to obtain the normal and shear stresses for that fault. We assumed the friction coefficient of 0.3, and defined the change to promote thrust faulting as positive. ΔCFS was 3.8 kPa for the earthquake (1), and was −2.8 kPa for (2). They were less than 1 kPa for (3) and (4).

[31] If we consider a slip of 6 cm of a fault as wide as 60 km, the stress drop is ~800 kPa (rigidity was assumed as 40 GPa). Assuming the biannual recurrence of the events, the daily build-up of the stress would be 4–5 kPa. Therefore even the largest stress disturbance by these earthquakes does not exceed the daily stress increase, and it is unlikely that these earthquakes affected the recurrence rhythm. In fact, the earthquake (1) does not disturb the rhythm at all. In Figure 7c, the earthquake (2) appears to have delayed the 9th SSE, and this is qualitatively consistent with its negative ΔCFS. However, close inspection of Figure 7c suggests that the 8th SSE, well before this earthquake, already delayed, and
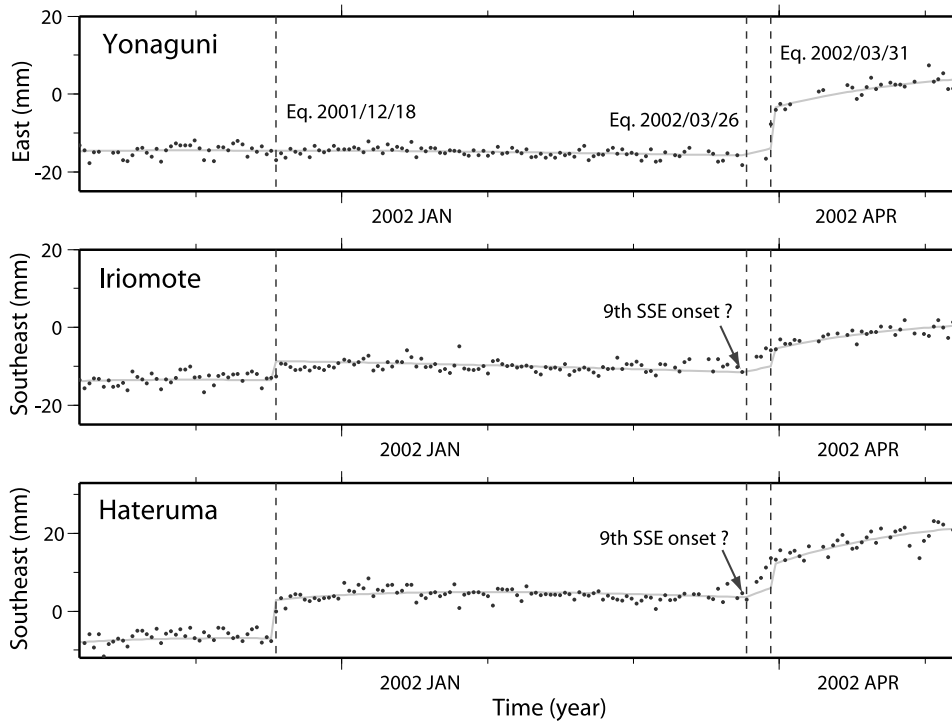
Figure 9. Movements of three GPS stations from November 2001 to May 2002 relative to Miyako. Vertical dashed lines show the earthquakes in Figure 8. Yonaguni shows coseismic movements associated with the 31 March 2002 earthquake, but the other two stations do not. On the other hand, Iriomote and Hateruma show coseismic movements in the 18 December 2001 earthquake while Yonaguni does not. The 9th SSE seems to have started simultaneously with the 26 March 2002 earthquake.

reason for the delays should be therefore sought somewhere else.

[32] The 9th SSE seems to start simultaneously with the earthquake (3), which has positive ΔCFS. However, it is too small (less than 1 kPa) to let this earthquake play such a role. The interval between the 8th and 9th SSE is approximately one-half year, and the synchronism of the 9th SSE and the earthquake (3) would be a mere coincidence. Apart
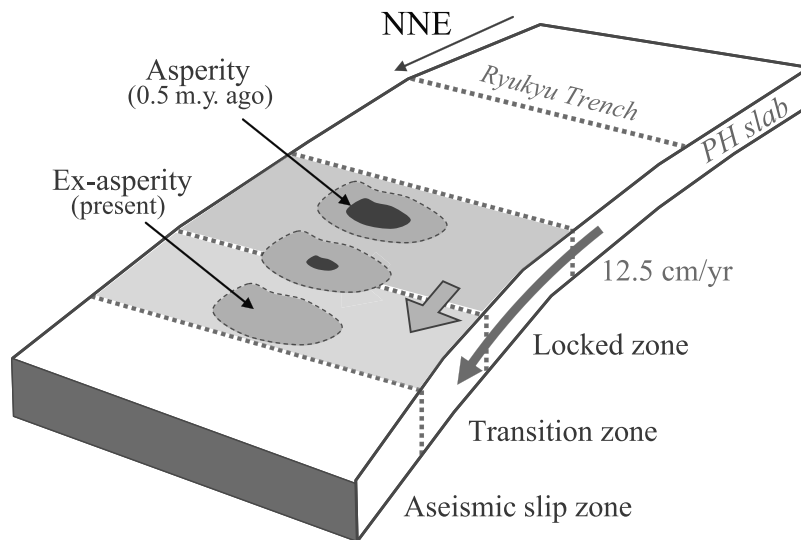

Figure 10. An image of alteration of an asperity on the PH slab subducting beneath SR at the Ryukyu Trench. The strongly coupled unstable part (asperity, shown in dark gray) was surrounded by the conditionally stable part (light gray) which was normally coupled but moved slowly following the fast rupture in the asperity. The unstable part became smaller as the slab subducted to a deeper part and ambient temperature increases. The unstable part eventually disappeared, and the whole part slips episodically but aseismically now.

from seismic triggering, there are several indications that non-volcanic deep tremor activities correlate with semi-diurnal and diurnal tide [*Rubinstein et al.*, 2008]. Because it is difficult to constrain the onset time of SSE with time resolution better than a few days, we here do not discuss tidal triggering of SSE in Ryukyu.

5.2. Iriomote Ex-Asperity

[33] A large difference between SSE in the present case and those in Shikoku and Cascadia is the existence of interplate thrust earthquakes around the slow-slip region. Large historical thrust earthquakes have occurred in the Nankai Trough south of Shikoku with an average interval of 120 years [*Sangawa*, 1993]. In Cascadia, the last large thrust earthquake occurred in 1700 [*Satake et al.*, 1998].

[34] In the Ryukyu Arc to the south of SR, there are no large thrust events (and no interplate coupling) except the biannual SSE studied here. There was an M7.4 earthquake in 1771 that killed half of the Ishigaki Island population by one of the largest historical tsunamis in Japan (the Yaeyama earthquake tsunami). A recent study suggested that this is not an interplate earthquake at the Ryukyu Trench, but has occurred in a shallow normal fault striking perpendicular to the arc to the east of the island [*Nakamura*, 2006]. At the Japan Trench east of the NE Japan Arc small repeating earthquakes occur, i.e., regularly repeating ruptures of small isolated asperities in a steadily sliding zone [*Matsuzawa et al.*, 2002; *Okada et al.*, 2003]. Considering mechanical isolation, the SR SSE resembles such small repeaters rather than SSE in Shikoku or ETS in Cascadia.

[35] An asperity is a part in the plate interface with stronger coupling than the surrounding area. Large thrust earthquakes nucleate there when an asperity is in a seismogenic depth; shallower part involves poorly consolidated materials that slide steadily, and in the lower part high temperature enables ductile flow of minerals and stable subduction [*Scholz*, 1998]. Such asperities in the seismogenic zone have been mapped along the Japan Trench by *Yamanaka and Kikuchi* [2004]. An asperity is recognized in geodesy as the region showing large slip in coseismic slip distribution on the plate interface recovered using GPS site displacements. It also coincides with the region with large slip deficit inferred by inverting interseismic velocities. In the Southwest Honshu Arc, interseismic velocity fields suggested that large slip deficits exist at depths 5–25 km, and they decay downward and disappear at around 35 km [*Miyazaki and Heki*, 2001].

[36] In the seismogenic depths, fast rupture of an asperity in thrust interplate earthquake is often followed by the postseismic slow slip (afterslip) in areas surrounding the asperity [*Yagi et al.*, 2003]. The SSE in the Ryukyu Arc seems to happen in an area that once was an asperity. As an asperity subducts to a greater depth, increasing ambient temperature would stabilize the slip and the proportion of the fast rupture segment to the afterslip segment would decrease. The entire asperity would eventually come to a state of slipping episodically but only slowly (Figure 10). Here we call it the "Iriomote ex-asperity", because it lies beneath the Iriomote Island (Figure 4). Although it slips only slowly now, its behavior still resembles an asperity, e.g., quasi-periodic recurrences. As suggested by *Shimazaki and Nakata* [1980] for the Nankai Earthquakes, ex-asperities may

have the common feature to recur with time-predictable nature. One remaining mystery is that there are no "live" asperities at the Ryukyu Trench. It is not clear, at the moment, whether this reflects the lack of subducting seamounts (a candidate for origin of asperities) or essential differences in physical properties of the plate interface from other subduction zones with asperities.

[37] There the subduction is rather fast (12.5 cm/yr means 125 km/Ma), and it was less than one million years ago that this ex-asperity was in the middle of the seismogenic zone. If this ex-asperity had caused fast ruptures there, M8 class large earthquakes might have occurred once in a few tens of years with devastating tsunamis in these islands. It would be interesting to look for geological evidence of such ancient large thrust earthquakes in the Ryukyu Arc.

References

Argus, D. F., and R. G. Gordon (1991), No-net-rotation model of current plate velocities incorporating plate motion model NUVEL-1, *Geophys. Res. Lett.*, *18*, 2039–2042.

Dragert, H., K. Wang, and T. S. James (2001), A silent slip event on the deeper Cascadia subduction interface, *Science*, *292*, 1525–1528.

Dragert, H., K. Wang, and G. Rogers (2004), Geodetic and seismic signatures of episodic tremor and slip in northern Cascadia subduction zone, *Earth Planets Space*, *56*, 1143–1150.

Heki, K. (2007), Secular, transient and seasonal crustal movements in Japan from a dense GPS array: Implication for plate dynamics in convergent boundaries, in *The Seismogenic Zone of Subduction Thrust Faults* edited by T. Dixon and C. Moore, pp. 512–539, Columbia Univ. Press, New York.

Heki, K., S. Miyazaki, and H. Tsuji (1997), Silent fault slip following an interplate thrust earthquake at the Japan Trench, *Nature*, *386*, 595–597.

Hirose, H., and K. Obara (2005), Repeating short- and long-term slow slip events with deep tremor activity around the Bungo Channel region, southwest Japan, *Earth Planets Space*, *57*, 961–972.

Hirose, H., K. Hirahara, F. Kimata, N. Fujii, and S. Miyazaki (1999), A slow thrust slip event following the two 1996 Hyuganada earthquakes beneath the Bungo Channel, Southwest Japan, *Geophys. Res. Lett.*, *26*(21), 3237–3240.

Ide, S., G. C. Beroza, D. R. Shelly, and T. Uchide (2007), A scaling law for slow earthquakes, *Nature*, *447*, 76–79.

Ito, Y., K. Obara, K. Shiomi, S. Sekine, and H. Hirose (2006), Slow earthquakes coincident with episodic tremors and slow slip events, *Science*, *26*, 503–506.

Kostoglodov, V., S. K. Singh, J. A. Santiago, S. I. Franco, K. M. Larson, A. R. Lowry, and R. Bilham (2003), A large silent earthquake in the Guerrero seismic gap, Mexico, *Geophys. Res. Lett.*, *30*(15), 1807, doi:10.1029/2003GL017219.

Lowry, A. R. (2006), Resonant slow fault slip in subduction zones forced by climatic load stress, *Nature*, *442*, 802–805.

Lowry, A. R., K. M. Larson, V. Kostoglodov, and R. Bilham (2001), Transient fault slip in Guerrero, southern Mexico, *Geophys. Res. Lett.*, *28*(19), 3753–3756.

Matsuzawa, T., T. Igarashi, and A. Hasegawa (2002), Characteristic small-earthquake sequence off Sanriku, northeastern Honshu, Japan, *Geophys. Res. Lett.*, *29*(11), 1543, doi:10.1029/2001GL014632.

Miller, M. M., T. Melbourne, D. J. Johnson, and W. Q. Summer (2002), Periodic slow earthquakes from the Cascadia subduction zone, *Science*, *295*, 2423.

Miyazaki, S., and K. Heki (2001), Crustal velocity field of Southwest Japan: Subduction and arc-arc collision, *J. Geophys. Res.*, *106*(B3), 4305–4326.

Nakamura, M. (2006), Source fault model of the 1771 Yaeyama Tsunami, Southern Ryukyu Islands, Japan, inferred from numerical simulation, *Pure Appl. Geophys.*, *163*, 41–54.

Nishimura, S., M. Hashimoto, and M. Ando (2004), A rigid block rotation model for the GPS derived velocity field along the Ryukyu arc, *Phys. Earth Planet. Inter.*, *142*, 185–203.

Obara, K. (2002), Nonvolcanic deep tremor associated with subduction in southwest Japan, *Science*, *296*, 1579–1681.

Obara, K., H. Hirose, F. Yamamizu, and K. Kasahara (2004), Episodic slow slip events accompanied by non-volcanic tremors in southwest Japan

subduction zone, *Geophys. Res. Lett.*, *31*, L23602, doi:10.1029/2004GL020848.

Ohta, Y., J. Freymueller, and S. Miura (2007), The time constant variations of slow slip events in the south Alaska subduction zone, paper presented at the 2007 Fall Meeting of American Geophysical Union, San Francisco.

Okada, Y. (1992), Internal deformation due to shear and tensile faults in a half-space, *Bull. Seismol. Soc. Am.*, *82*, 1018–1040.

Okada, T., T. Matsuzawa, and A. Hasegawa (2003), Comparison of source areas of M4.8 ± 0.1 repeating earthquakes off Kamaishi, NE Japan: Are asperities persistent features?, *Earth Planet. Sci. Lett.*, *213*, 361–374.

Ozawa, S., M. Murakami, M. Kaidzu, T. Tada, T. Sagiya, Y. Hatanaka, H. Yarai, and T. Nishimura (2002), Detection and monitoring of ongoing aseismic slip in the Tokai Region, central Japan, *Science*, *298*, 1009–1012.

Ozawa, S., S. Miyazaki, Y. Hatanaka, T. Imakiire, M. Kaidzu, and M. Murakami (2003), Characteristic silent earthquakes in the eastern part of the Boso Peninsula, central Japan, *Geophys. Res. Lett.*, *30*(6), 1283, doi:10.1029/2002GL016665.

Ozawa, S., H. Suito, and M. Tobita (2007), Occurrence of quasi-periodic slow-slip off the east coast of the Boso Peninsula, central Japan, *Earth Planets Space*, *59*, 1241–1245.

Rogers, G., and H. Dragert (2003), Episodic tremor and slip on the Cascadia subduction zone: The chatter of silent slip, *Science*, *300*, 1942–1943.

Rubinstein, J. L., M. La Rocca, J. E. Vidale, C. Creager, and A. G. Wech (2008), Tidal modulation of nonvolcanic tremor, *Science*, *319*, 186–189, doi:10.1126/science.1150558.

Sagiya, T. (2004), Interplate coupling in the Kanto District, central Japan, and the Boso Peninsula silent earthquake in May 1996, *Pure Appl. Geophys.*, *161*, 2327–2342.

Sangawa, A. (1993), The paleo-earthquake study using traces of the liquifaction, *Quat. Res.*, *32*, 249–255, (in Japanese).

Satake, K., K. Shimazaki, Y. Tsuji, and K. Ueda (1998), Time and size of a giant earthquake in Cascadia inferred from Japanese tsunami records of January 1700, *Nature*, *379*, 246–249, 1996.

Scholz, C. H. (1998), Earthquakes and friction laws, *Nature*, *391*, 37–41.

Shen, Z.-K., Q. Wang, R. Bürgmann, Y. Wan, and J. Ning (2005), Pole-tide modulation of slow slip events at Circum-Pacific subduction zones, *Bull. Seismol. Soc. Am.*, *95*, 2009–2015.

Shimazaki, K., and T. Nakata (1980), Time-predictable recurrence model for large earthquakes, *Geophys. Res. Lett.*, *7*(4), 279–282.

Sibuet, J.-C., B. Deffontaines, S. Hsu, N. Thareau, J. Le Formal, and C. Liu (1998), Okinawa trough backarc basin: Earth tectonic and magmatic evolution, *J. Geophys. Res.*, *103*(B12), 30,245–30,267.

Takahashi, H., et al. (2004), GPS observation of the first month of postseismic crustal deformation associated with the 2003 Tokachi-oki earthquake (M_{JMA} 8.0), off southeastern Hokkaido, Japan, *Earth Planets Space*, *56*, 377–382.

Yagi, Y., M. Kikuchi, and T. Nishimura (2003), Co-seismic slip, post-seismic slip, and largest aftershock associated with the 1994 Sanriku-haruka-oki, Japan, earthquake, *Geophys. Res. Lett.*, *30*(22), 2177, doi:10.1029/2003GL018189.

Yamamoto, E., S. Matsumura, and T. Ohkubo (2003), The slow slip event in the Tokai region, detected by tilt and seismic observation—Possible recurrence, paper presented at the 2003 Fall Meeting of the Seism. Soc. Japan, Kyoto, Japan, 8 Oct.

Yamanaka, Y., and M. Kikuchi (2004), Asperity map along the subduction zone in northeastern Japan inferred from regional seismic data, *J. Geophys. Res.*, *109*, B07307, doi:10.1029/2003JB002683.

Yarai, H., H. Munekane, and T. Nishimura (2004), Repeating slow slip events south off the Yaeyama Islands, paper presented at the 2004 Fall Meeting of the Geodetic Society of Japan, Tokyo.

Yu, S.-B., L.-C. Kuo, R. S. Punongbayan, and E. G. Ramos (1999), GPS observation of crustal deformation in the Taiwan-Luzon region, *Geophys. Res. Lett.*, *26*(7), 923–926.

———————————

K. Heki and T. Kataoka, Department of Natural History Sciences, Hokkaido University, N10 W8, Kita-ku, Sapporo, Hokkaido 060-0810, Japan. (heki@mail.sci.hokudai.ac.jp)